



Four years (2011-2015) of Total Gaseous Mercury measurements from the Cape Verde Atmospheric Observatory

Katie A Read¹, Luis M Neves², Lucy J Carpenter¹, Alastair C Lewis¹, Zoe Fleming³, and John Kentisbeer⁴

¹National Centre for Atmospheric Science (NCAS), Department of Chemistry, University of York, York, YO10 5DD, UK

²Instituto Nacional de Meteorologia Geofisica (INMG), Delegação de São Vicente, Monte, CP15, Mindelo, Rep of Cape Verde

³National Centre for Atmospheric Science (NCAS), University of Leicester, Leicester, LE1 7RH, UK

⁴Centre for Ecology and Hydrology (CEH), Bush Estate, Penicuik, Midlothian, EH26 0QB, UK

Correspondence to: Katie A. Read (katie.read@york.ac.uk)

Abstract. Mercury is a chemical with widespread anthropogenic emissions that is known to be highly toxic to humans, ecosystems and wildlife. Global anthropogenic emissions are around 20% higher than natural emissions and the amount of mercury released into the atmosphere has increased since the industrial revolution. In 2005 the European Union and United States adopted measures to reduce mercury use, in part to offset the impacts of increasing emissions in industrialising countries. The changing regional emissions of mercury have impacts on a range of spatial scales. Here we report four years (Dec 2011 – Dec 2015) of Total Gaseous Mercury (TGM) measurements at the Cape Verde Observatory (CVO), a global WMO-GAW station located in the sub-tropical remote marine boundary layer. Observed total gaseous mercury concentrations were between 1.03 and 1.33 ng m⁻³ (10th, 90th percentiles), close to expectations based on previous interhemispheric gradient measurements. We observe a decreasing trend in TGM (0.04 ± 0.03 ng m⁻³ yr⁻¹, $-3.4\% \pm 2.4\%$ yr⁻¹) over the four years consistent with the reported decrease of mercury concentrations in North Atlantic surface waters and reductions in anthropogenic emissions. The trend was more visible in the summer (Jul-Sep) than in the winter (Dec-Feb), when measurements were impacted by air from the African continent and Sahara/Sahel regions. African air masses were also associated with the highest and most variable TGM concentrations. We suggest that the less pronounced downward trend in African air may be attributed to poorly controlled anthropogenic sources such as artisanal and small-scale gold mining (ASGM).

1 Introduction

Mercury is present in the atmosphere in three main forms; gaseous elemental mercury Hg⁰, which is the most common form in the gas phase, oxidized mercury Hg^{II} (GOM or RGM), and Hg-bound to particulate matter (PBM). The measurement of Total Gaseous Mercury (TGM or GEM) encompasses the measurement of all of these forms with Hg⁰ contributing to around 90-99% of the total Hg or TGM.

Anthropogenic sources of mercury account for around 30% of the total amount and include emissions from coal burning, mining, cement production, oil refining and waste incineration. Hg⁰ reacts slowly with atmospheric oxidants, with a global lifetime of around 6-8 months (Selin et al., 2007; Holmes et al., 2010), and so can be transported to remote regions. When oxidized to less volatile Hg^{II}, it can be deposited either through wet deposition processes (precipitation-scavenging) or by surface uptake (Gustin et al., 2012; Schroeder and Munthe, 1998; Sather et al., 2013; Wright et al., 2014). Hg⁰ also undergoes slow dry deposition of mercury through air-surface exchange with both terrestrial and aquatic surfaces (Zhang et al., 2009; Wang et al., 2016). Once deposited, transformation to highly toxic species such as the neurotoxic methylmercury allows bioaccumulation in food chains and thus poses a health risk to humans and a damaging effect to ecosystems (US EPA, 1997). Previously deposited mercury can also be reduced back to Hg⁰ through the natural weathering of mercury-containing rocks, geothermal activity, or from volcanic activity, and then re-emitted back to the atmosphere (Gustin et al., 2012)(Qureshi, 2012).

Reactions of Hg⁰ to Hg^{II} with the hydroxyl radical (OH) and ozone (O₃) were historically accepted as the dominant photochemical oxidation mechanisms (Bergan and Rodhe, 2001; Lin et al., 2006; Seigneur



et al., 2006; Selin et al., 2007; Pongprueksa et al., 2008). Recent work has suggested that there may be significant other oxidants such as atomic halogens (Holmes et al., 2010; Wang et al., 2014) and more complex two-step oxidation schemes, which include further reactions with NO_2 and HO_2 , however the kinetics are highly uncertain (Goodsite et al., 2004) (Goodsite et al., 2004; Holmes et al., 2010). Heterogeneous oxidation in clouds may also contribute but is not experimentally proven (Ariya et al., 2009; Calvert and Lindberg, 2005).

Strode et al. (2007) estimated that 36% of all mercury emissions in the northern hemisphere come from the ocean both through primary emission (ocean upwelling and mercury-containing rocks) and from re-emission of previously deposited mercury (as Hg^{II}), but this increases to 55% as you move into the southern hemisphere (Strode et al., 2007). The major anthropogenic source affecting the remote marine boundary layer is likely to be long-range transport of Hg^0 from coal-fired combustion (smelting, waste incineration, chemical plants) rather than from Hg^{II} , which is more likely to deposit regionally due to its relatively short lifetime of 4.8 hours (Zhang et al., 2012). Other industrial sources for Hg include artisanal and small-scale gold mining (ASGM), which are known to occur in West Africa (Telmer and Velga, 2009; UNEP, 2013) and will likely regionally influence the measurements described here. For the 2013 UNEP global assessment, ASGM emission data were compiled from field and industry reports but with an uncertainty of ca. $\pm 43\%$ due to the multitude and varying nature of ASGM sites. In recent years, global emissions from ASGM, and in particular the proportion of global emissions attributed to South America and Sub-Saharan Africa, appear to be increasing; however this assumption may be due to improved reporting (Muntean et al., 2014). The majority of global anthropogenic emissions of Hg to the atmosphere in 2010 are associated with ASGM (37%), with one third thought to be from sub-saharan Africa (UNEP, 2013).

A community strategy developed by the EU was adopted in 2005 and listed 20 actions to reduce mercury emissions, cut mercury supply and demand, and to protect people against exposure. This strategy had a strong focus on the need to take a global approach and included actions relating to multilateral negotiations for the conclusion of a legally binding convention on mercury (http://ec.europa.eu/environment/chemicals/mercury/strategy_en.htm). The UNEP Global Mercury partnership led by the US Environmental Protection Agency took a similar approach (<http://www.unep.org/chemicalsandwaste/Metals/GlobalMercuryPartnership/tabid/1253/Default.aspx>) and these initiatives formed the basis of the Minamata Convention on Mercury, which was agreed in 2013 and is a global treaty to protect human health and the environment from the adverse effects of mercury (<http://www.mercuryconvention.org/>).

It has been a source of contradiction that in the northern hemisphere, while both measured atmospheric Hg concentrations and wet deposition fluxes have been decreasing since 1990 (Soerensen et al., 2012) and 1996–2013 (Slemr et al., 2013; Weigelt et al., 2015); global Hg emissions during this period were calculated to be increasing (Pacyna et al., 2010; Streets et al., 2011). Very recently, however, Zhang et al., (2016), using a revised inventory and the global model GEOS-CHEM, have shown that global Hg emissions may also be decreasing. They suggest that a large discrepancy in the emissions data was from locally deposited mercury close to coal-fired utilities. It is thought that this source has declined more rapidly than was previously predicted due to shifts in mercury speciation from air pollution control technology targeted at SO_2 and NO_x (Zhang et al., 2016). Flue gas desulfurization (FGD) - which controls SO_2 emissions - washes out Hg^{II} , whilst selective catalytic reduction (SCR) to control NO_x emissions also oxidises Hg^0 to Hg^{II} . These effects of FGD, in addition to the recent phase-out of Hg from commercial products (UNEP Minamata Convention on Mercury) and lower global estimates from small-scale gold mining, serve to explain the globally decreasing atmospheric concentrations in the model. Zhang et al. (2016) also found that the larger emission decreases observed in North America and Europe globally offset the increases from other major polluted regions e.g. from coal-fired utilities in East Asia (Pacyna et al., 2010; Pirrone et al., 2013).

Using data from ship cruises, Soerensen et al. (2012) observed a significant decreasing trend of atmospheric mercury concentrations over the North Atlantic of $-0.046 \text{ ng m}^{-3} \text{ yr}^{-1}$ ($-2.5\% \text{ yr}^{-1}$), with smaller trends at more southern latitudes (Soerensen et al., 2012). They suggest that this decline is due to decreasing oceanic evasion driven by declining subsurface water Hg^0 concentrations ($-5.7\% \text{ yr}^{-1}$ since 1999, (Mason et al., 2012)).

Here we report four years (Dec 2011 – Dec 2015) of TGM measurements at the Cape Verde Observatory (CVO), a clean marine background station located in the subtropical Atlantic. The



measurements presented here are part of the EU Global Mercury Observation System (GMOS) network. The GMOS network of sites was established in 2011 with the aim of addressing known gaps in the spatial and temporal measurement of mercury, as well as improving knowledge of Hg speciation. The data is being used to validate regional and global scale atmospheric Hg models in order to improve understanding of global Hg transport, deposition and re-emission as well as providing a contribution to future international policy development and implementation (www.gmos.eu).

2 Experimental

The CVO was established in 2006 as a multilateral project between the UK, Germany and Republic of Cape Verde. Long-term atmospheric measurements include reactive trace gases including ozone, carbon monoxide, nitrogen oxides and volatile organic compounds (National Centre for Atmospheric Sciences (NCAS), University of York, UK), long lived greenhouse gases (Max-Planck Institute (MPI), Jena, Germany), and physical and chemical characterisation of aerosol (Leibniz Institute for Tropospheric Research (TROPOS), Leipzig, Germany). Details of the measurements and characteristics of the station can be found in Carpenter et al., (2010).

The CVO is positioned on the northeast side of Sao Vicente (16.85°N, 24.87°W), one of ten islands in the Cape Verde archipelago (Fig. 1). The island is of volcanic origin and the CVO is situated 50m from the coastline. The climate is warm (mean annual air temperature is $24.0^{\circ}\text{C} \pm 2.0^{\circ}\text{C}$) and dry with extremely low annual rainfall (<200 mm), which occurs mostly during the rainy season of July–November. The site receives air masses from the northeasterly trade winds for 95% of the time, which have travelled typically for five days over the ocean. Research flights carried out over the CVO in summer 2007 established that the boundary layer is well mixed (Read et al., 2008). There is no coastal shelf to the island at this location point, and the CVO conditions are considered to be representative of the North Atlantic open ocean boundary layer.

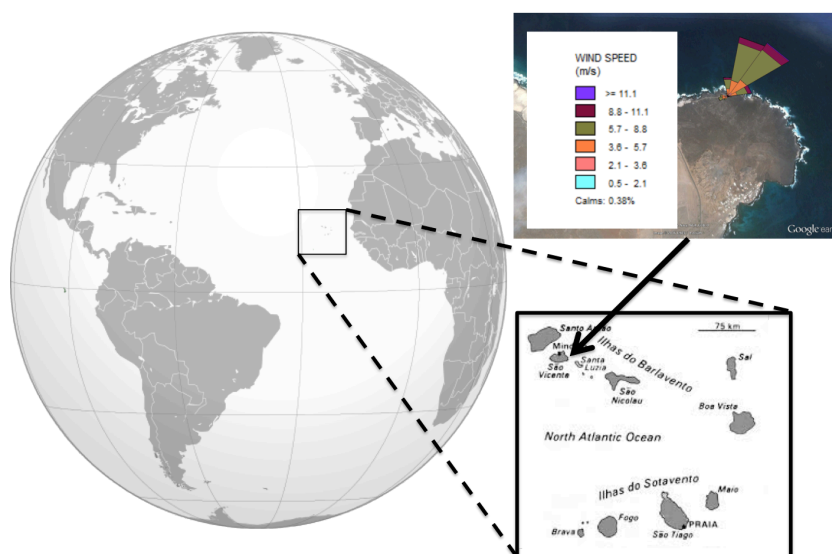


Figure 1: Cape Verde site location. Top right, image from Google earth: V7.1.5.1557 (6th July 2016). São Vicente, Cape Verde, 16°51'59.60"N, 24° 52'03.60"W, Eye altitude 2.70 km. Wind rose for the measurement period is coloured by wind speed.

Air is sampled from the main laboratory glass manifold (10 m, 2" diameter, residence time 4 seconds) and then through a 2 m length of 1/4" Teflon tubing and a particulate filter which is changed every two months. The entire inlet is heated. A TEKRA 2537B analyser (Tekran Inc., Toronto, Canada) was used for the TGM measurements and is described in detail elsewhere (Steffen et al., 2014) and so only a brief summary is presented here. The analytical principle collects the TGM onto gold traps with subsequent thermal desorption and detection by atomic fluorescence spectroscopy ($\lambda = 253.7$ nm,



(Bloom and Fitzgerald, 1988)). Samples of 5 L volume are obtained every 5 minutes (1 L min⁻¹ flow rate) with a detection limit of around 0.1 ng m⁻³, using a dual trap set-up. Calibrations are performed every 72 hours using an internal mercury permeation source which injects a known amount of Hg⁰ into mercury-free zero air (using a TEKRAN Zero Air filter, part no: 90-25360-00). The calibration consists of a zero and a span on each channel. The effective span was 19.08 ng m⁻³ for a sample volume of 5 L. The permeation rate was externally validated using manual injections of saturated mercury vapour taken from a Tekran 2505 mercury vapour calibration unit and after 5 years found to be within 3.58% of the instrumental set-point. The detection limit of the instrument was 0.1 ng m⁻³.

Four years of data are presented here obtained between 5th December 2011 and 5th December 2015. In calculating annual trends and averages, we have used data from 1 Dec – 30 Nov. The data was quality controlled using the central GMOS-Data Quality Management (G-DQM) system (Cinnirella et al., 2014; D'Amore et al., 2015). The G-DQM allows harmonization of data across the network and is able to acquire and process data in near real time allowing immediate diagnosis of issues. It was developed using harmonized Standard Operating Procedures, which had been established over many years by European and Canadian monitoring networks, together with recent literature (Brown et al., 2010; Gay et al., 2013; Steffen et al., 2012). An additional filter has been applied to the data presented here to exclude periods when the relative humidity was higher than 90%, as the data was prone to increased uncertainties due to water condensing in the instrument. Instrument issues led to some significant data gaps; a lamp failure caused major data gaps between July-August 2012 and May-June 2014, whilst a pump failure caused downtime between October 2012-January 2013.

3 Results and discussion

3.1 Statistics and seasonal cycles

The mean TGM concentration over 2011-2015 was 1.191 ± 0.128 ng m⁻³ and the four-year time-series is shown in Fig. 2. Sprovieri et al. (2016) showed that the CVO measurements (site referred to as CAL rather than CVO) fit well within the north-south gradient of TGM data. Other sites of reference, which receive background air similar in origin to CVO, include Mace Head, Ireland, Nieuw Nickerie, Suriname, and Cape Point, South Africa (Table 1). The remoteness of the CVO is reflected in the small variability of the TGM measurements, compared to other sites.

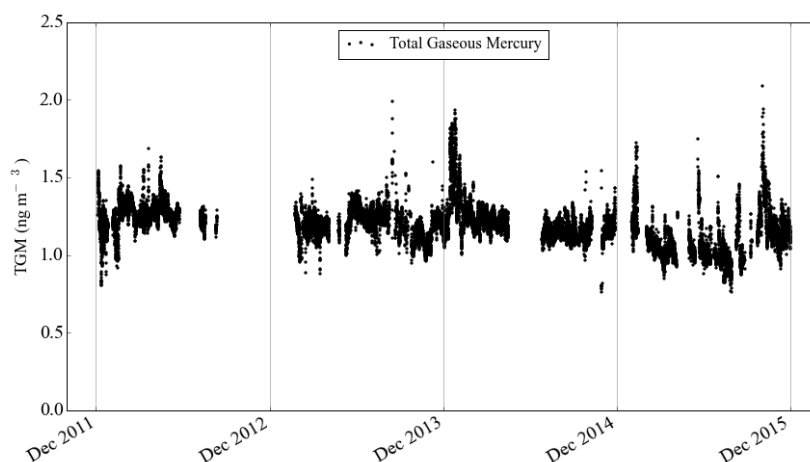


Figure 2: Time-series (December 2011-December 2015) of TGM data measured at the Cape Verde Observatory.

The data shown in Table 1 illustrate the dominating effect of emissions from the northern hemisphere compared to the southern hemisphere, with Mace Head (53°20'N, 9°54'W) TGM concentrations averaging 7-9% higher than those observed at Cape Point. The site at Nieuw Nickerie experiences 10% higher concentrations in the air arriving from the north compared to the south (Muller et al., 2012) and is additionally impacted by emissions from biomass burning and gold mining from South America



(Sprovieri et al., 2010). Comparisons to ship-borne field campaigns in the Atlantic made between 1977 and 2001 (Sprovieri et al., 2010) show that the data from CVO are more comparable with southern Atlantic conditions than the northern Atlantic.

| Site (Latitude, Longitude) | Average \pm standard deviation for 2013 (ng m ⁻³) | Average \pm standard deviation for 2014 (ng m ⁻³) |
|---|---|---|
| Mace Head, Ireland (53°20'N, 9°54'W) | 1.46 \pm 0.17 | 1.41 \pm 0.14 |
| Calhau, Rep of Cape Verde (16°51'N, 24°52'W) | 1.22 \pm 0.14 | 1.20 \pm 0.09 |
| Nieuw Nickerie, Suriname (5°56'N, 56° 59'W) | 1.13 \pm 0.42 | 1.28 \pm 0.46 |
| Cape Point, South Africa (33° 56'S, 18°28'E) | 1.03 \pm 0.11 | 1.09 \pm 0.12 |

Table 1. Average TGM concentrations and standard deviation statistics from comparable sites in 2013 and 2014. Data from Sprovieri et al., (2016).

The CVO TGM data shows a weak seasonal cycle (1.289 \pm 0.134 ng m⁻³ December maximum, 1.130 \pm 0.128 ng m⁻³ June minimum, Fig. 3) with generally higher concentrations in winter and lower in summer. This cycle is similar to that observed within sub-tropical maritime air masses at Mace Head, which is shallower than for other air masses (Weigelt et al., 2015) and generally not so defined as that of other remote sites in the Northern Hemisphere (Temme et al., 2007; Holmes et al., 2010). Selin et al., (2007) show that the mean seasonal amplitude of 12 northern mid-latitude sites between the maximum in January (winter) and minimum August (summer) is 0.19 ng m⁻³, compared to the CVO amplitude of 0.14 ng m⁻³ (December-June). A smaller seasonal cycle may mean that O₃ plays a more dominant role in the oxidation of Hg⁰ compared to other oxidants such as OH (Temme et al., 2007; Selin et al., 2007; Holmes et al., 2010). The equatorial nature of the CVO site means that solar irradiance and water vapour are high year-round (Carpenter et al., 2010; Whalley et al., 2010). This may lead to a less pronounced change in oxidation capacity between summer and winter, when compared to sites at higher latitudes.

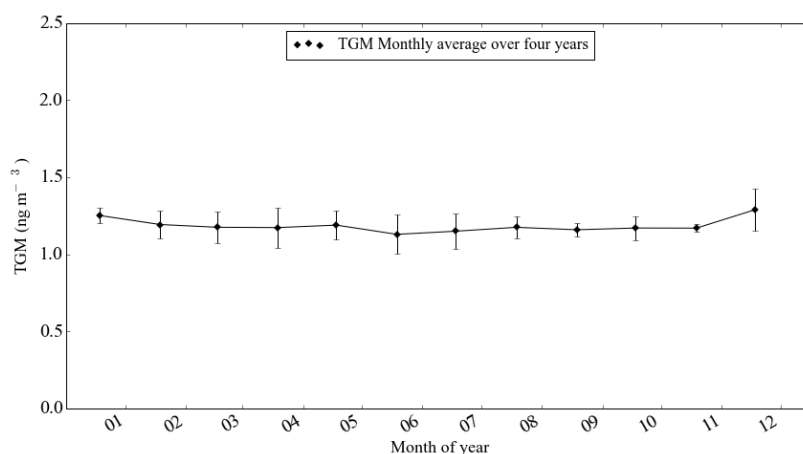


Figure 3: Seasonal cycle of TGM at CVO.

Anthropogenic emissions of mercury affecting the Atlantic region include emissions from coal combustion, which tend to have maximum impact in February-March due to a dominance of air from North America when fossil fuel consumption is highest (Duncan et al., 2007). This is additionally observed in the seasonal distribution of anthropogenic tracers such as carbon monoxide (Selin et al., 2007; Weigelt et al., 2015; Read et al., 2009). Ocean emissions of Hg⁰ from the reduction of Hg_{aq}^{II} to Hg_{aq}⁰, driven by increased biological production are at a maximum in June in the NH but December in



the SH (Strode et al., 2007). The seasonal trend may also be affected by meteorological differences in seasonal circulation patterns and cycles in boundary layer heights, clouds, precipitation and dry deposition characteristics (Dastoor and Larocque, 2004; Selin et al., 2007).

3.2 Trends

Box and whisker plots of annual averages are shown in Fig. 4. Over four years the data shows a weak downward trend ($0.04 \pm 0.034 \text{ ng m}^{-3} \text{ yr}^{-1}$). This trend is more visible in the data collected during the Cape Verdean summer ($-0.077 \pm 0.055 \text{ ng m}^{-3} \text{ yr}^{-1}$ June–August, Fig. 4b) than in the winter ($-0.003 \pm 0.192 \text{ ng m}^{-3} \text{ yr}^{-1}$ in December–February, Fig. 4c). Previous studies have shown a stronger decreasing trend in air that has been influenced by anthropogenic emissions, for which there is more ready detection of the impact of regulation. The seasonal findings here imply that there are additional sources of mercury influencing the measurements with greater effect in the winter months compared to the summer months. This may be because the actual emissions of mercury (which themselves are decreasing more rapidly) are increased in winter e.g. those from residential burning or it may be because a mercury-rich air mass (which is not decreasing or decreasing less) is a more dominant contributor to the CVO air composition at that time of the year. One explanation is an emission source such as ASGM impacting on continental African originated air that is predominantly measured by the CVO in winter (Carpenter et al., 2010). Alternatively global oxidant concentrations (such as that of OH) may be increasing which would affect summer concentrations more than winter, but there is little evidence of this.

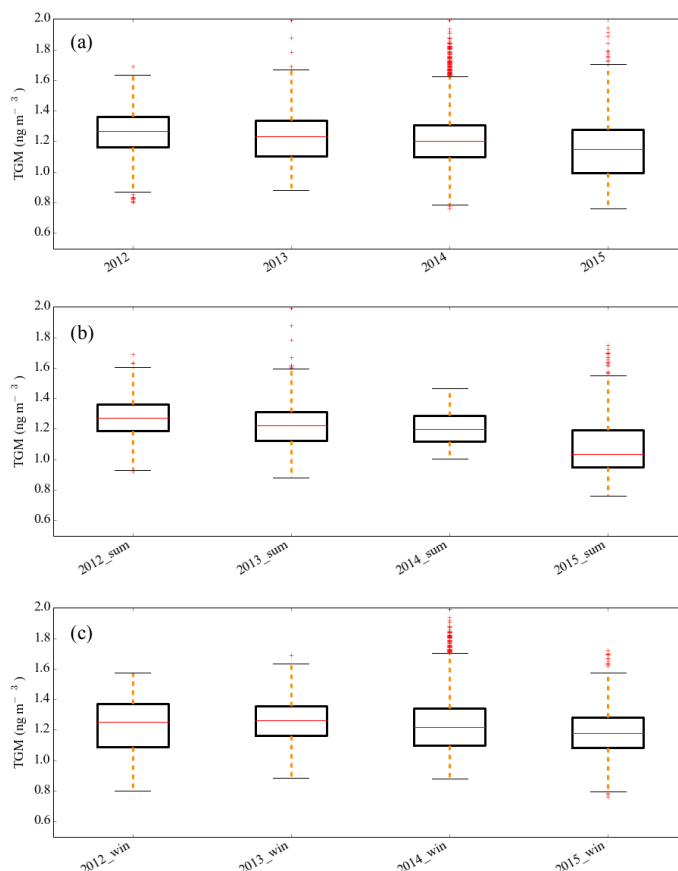


Figure 4: Box and whisker plots of a) annual data and separated by season b) summer, c) winter. The edges and middle of the boxes are 25th, 50th and 75th percentiles, 10th and 90th percentiles are illustrated by the spread of the whiskers.



In order to understand better the drivers of the TGM trends, data was classified according to the origin and pathways of airmasses arriving at the CVO over a ten-day period using the UK Met Office NAME dispersion model in passive tracer mode (Ryall et al., 2001). The air mass classifications have been used previously for evaluating the source regions of reactive trace gases arriving at CVO (Carpenter et al., 2010). Five geographical regions were defined (Coastal African, polluted Marine, Saharan Africa, Atlantic marine and Atlantic continental) and from these, 7 air mass types are classified based on the percentage time spent over each of the 5 regions (Carpenter et al., 2010). These are: Atlantic and African Coastal (AAC), Atlantic marine (AM), North American and Atlantic (NAA), North American and coastal African (NCA), European (with minimal African influence) (EUR), African (with minimal European influence) (AFR) and European and African (EUR/AFR).

Figure 5 shows histograms representing the data in each of the 7 classifications and Table 2 details the associated statistics. The highest and most variable concentrations of total gaseous mercury (mean was of $1.23 \pm 0.16 \text{ ng m}^{-3}$) were observed in the air from continental Africa (AFR). It has been established that West Africa is an important source region for ASGM activity (Telmer and Velga, 2009). It is difficult to determine whether West Africa is a growing source of emissions since data prior to these observations has been limited and is subject to large uncertainty. It is likely however that the ASGM emissions are less regulated than the anthropogenic emissions from coal combustion, ferrous/non-ferrous metal and cement production from Europe and the US (UNEP, 2013) and so is not decreasing in source strength. Selin et al., (2007) suggest that the global emission rate of anthropogenic mercury has declined by 5.5% and there is evidence from Northern Hemispheric sites, which are more impacted by anthropogenic emissions from these sources, that atmospheric concentrations are decreasing in-line with recent measures (Selin et al., 2007; Cole et al., 2014; Weigelt et al., 2015; Zhang et al., 2016).

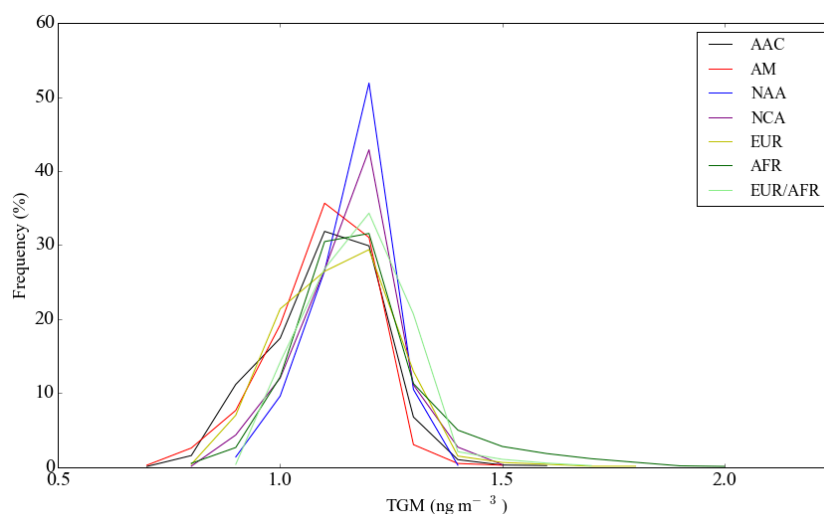


Figure 5: Histograms of air mass classified data.

| Air mass | Average \pm 1 sigma standard deviation (25 th -75 th percentiles) ng m^{-3} | % Time spent in air mass |
|----------|--|--------------------------|
| AAC | 1.14 \pm 0.11 (1.08-1.22) | 9% |
| AM | 1.15 \pm 0.12 (1.08-1.24) | 22% |
| NAA | 1.21 \pm 0.08 (1.17-1.27) | 17% |
| NCA | 1.20 \pm 0.10 (1.15-1.27) | 15% |
| EUR | 1.18 \pm 0.13 (1.08-1.26) | 7% |
| AFR | 1.23 \pm 0.16 (1.14-1.29) | 24% |
| EUR/AFR | 1.22 \pm 0.11 (1.16-1.30) | 6% |

Table 2. Statistics for the individual air mass classified data.



The lowest variability in TGM was observed in air that had travelled the longest periods since contact with continental sources even though these would have been subjected to greatest potential for ocean emissions (AM, NCA, NAA). The lowest concentrations ($1.144 \pm 0.109 \text{ ng m}^{-3}$) were observed in Atlantic and African coastal air (AAC).

The air was further separated by year to investigate whether the decreasing trend observed in the entire dataset could be seen within the individual air masses and if any further conclusions could be drawn.

The Theil-Sen function (Theil 1950; Sen 1968) was used to evaluate the 4-year trend based on monthly TGM averages and the results are shown in Fig. 6. In this function the slopes between all x, y pairs are calculated and the Theil-Sen estimate is then the median of all these slopes. The advantage of using this function is that it gives accurate confidence intervals and is resistant to outliers.

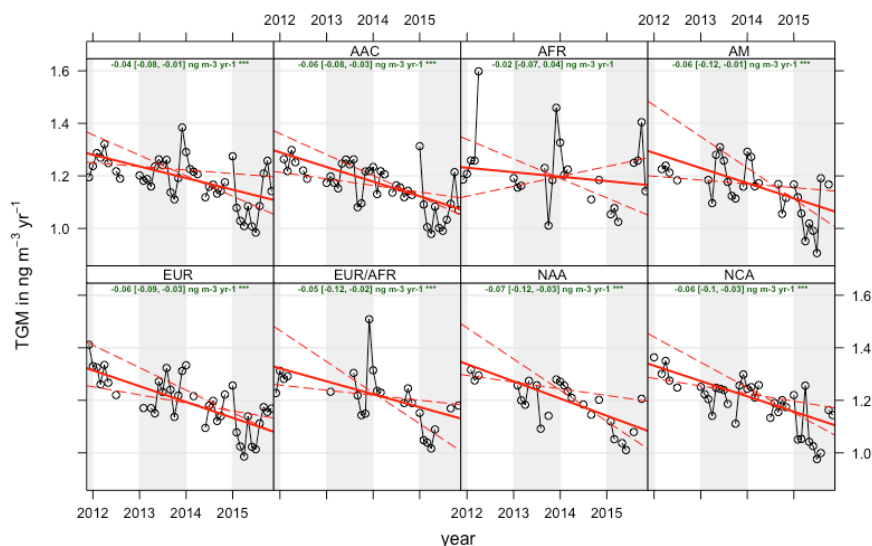


Figure 6: TGM trends separated by air mass at the Cape Verde Observatory. The green text shows the slope estimate and 95% confidence intervals in brackets.

The data for all air masses is shown in the top left panel with the rest of the panels showing the data separated by the seven air mass classifications. In each case the solid red line shows the trend estimate and the dashed red lines show the 95% confidence intervals for the trend based on resampling methods. The overall data show a trend of $-0.04 \text{ ng m}^{-3} \text{ yr}^{-1}$ (95% confidence interval of -0.07 to $-0.02 \text{ ng m}^{-3} \text{ yr}^{-1}$), as shown in the green text. The symbol “***” indicates that the trend is significant to the 0.001 level. Over the 4-year period the trends were (in $\text{ng m}^{-3} \text{ yr}^{-1}$): -0.06 , -0.02 , -0.06 , -0.06 , -0.05 , -0.07 , -0.06 for AAC, AFR, AM, EUR, EUR/AFR, NAA and NCA respectively. Only in the African (AFR) air is the trend not significant and suggests some additional input to the background concentrations. This would also explain the higher and more variable concentrations that we observe in this air mass.

Weigelt et al., (2015) observed an annual decrease in TGM concentrations at Mace Head ($53^{\circ}20'N$, $9^{\circ}54'W$, 10 m asl) of between -0.021 and $-0.023 \text{ ng m}^{-3} \text{ yr}^{-1}$ between 1996–2013, close to the upper confidence levels shown here (Weigelt et al., 2015). A global calculation using the GEOS-CHEM model (Soerensen et al., 2012) suggested that the TGM trend within sub-tropical maritime air masses (air from south of $28^{\circ}N$, west of $10^{\circ}W$) of $-0.016 \pm 0.002 \text{ ng m}^{-3} \text{ yr}^{-1}$ is lower than over the Northern Atlantic (model prediction of $-0.04 \text{ ng m}^{-3} \text{ yr}^{-1}$). In that evaluation an observed shallower decrease than the GEOS-CHEM prediction has been attributed to a shallower seasonal variation of oxidant concentrations in the region rather than to higher emissions (Weigelt et al., 2015). That research also suggests that the trend is leveling off in contrast to the findings presented here.



The overall trend (2011–2015) of $-0.04 \text{ ng m}^{-3} \text{ yr}^{-1}$ is in line with that calculated by Soerensen et al., (2012) from their measurements over the North Atlantic, whilst further south at Cape Point the trend for 17 years (1996–2013) was reported as $-0.018 \text{ ng m}^{-3} \text{ yr}^{-1}$ (95% significance interval of -0.035 to $-0.013 \text{ ng m}^{-3} \text{ yr}^{-1}$), lower than reported here but which may not take into account the very recent decreases in emissions (Weigelt et al., 2015; Soerensen et al., 2012).

3.3 Short term variability

The TGM data shows a very weak (statistically insignificant) diurnal profile in all air masses. Nevertheless, the maximum at night and minimum in early afternoon is consistent with the reaction with OH being the main loss term (Fig. 7), and similar to the diurnal profiles both in magnitude and shape that are presented in Wang et al., (2014) from measurements in the Pacific Ocean. The lowest concentrations and deepest diurnal amplitude (of 0.062 ng m^{-3}) observed at the CVO were in air that had spent more time over the ocean. The weakest diurnal cycle in TGM is observed in the AFR and EUR/AFR air masses (variation amplitudes of 0.028 ng m^{-3} and 0.036 ng m^{-3} respectively), consistent with fresh anthropogenic emissions influencing the concentrations (Wang et al., 2014).

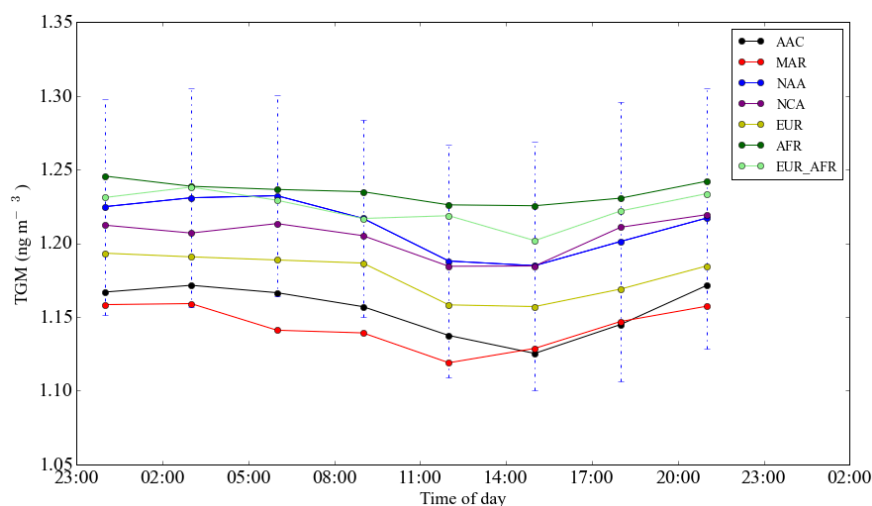


Figure 7: Diurnal variability of TGM separated by air mass. The error bars for data classified as from the North American and Atlantic (NAA) are included on the plot.

Rural sites tend to show minimum concentrations before sunrise and then maximum concentrations around noon (Lan et al., 2012; Nair et al., 2012). This is assumed to be due to the presence of a strong nocturnal boundary layer, which is then diluted by the vertical mixing of the boundary layer in the morning. Increased oxidation throughout the day at those locations leads to a decreasing or leveling off of TGM concentrations after noon. The results shown here suggest that the boundary layer effect is minimised at this location consistent with previous findings (Read et al., 2008; Carpenter et al., 2010).

4 Conclusions

We report a four-year decreasing trend in total gaseous mercury (TGM) concentrations over the subtropical north Atlantic of $-0.04 \pm 0.03 \text{ ng m}^{-3} \text{ yr}^{-1}$, a rate of decline that is in agreement with a number of other studies. A downward trend in concentration was observed in 6 out of 7 different air mass types, all associated broadly with long-range transport of air from the US and Europe over the north Atlantic ocean to the measurement location. The smallest and least significant downward trend ($-0.02 \pm 0.03 \text{ ng m}^{-3} \text{ yr}^{-1}$) was observed in air that was influenced by West Africa and the Sahel and Sahara, where emissions are less understood and may well be still increasing. The UNEP Global Mercury Assessment report in 2013 suggested that more work is needed to improve emissions estimates for West African sources including field measurements around ASGM sites.



Data availability

The data presented here is freely available at the Centre for Environmental Data Analysis (CEDA) at <http://catalogue.ceda.ac.uk/uuid/0ae5eb7ce3ad4885a7223dd7b69f4db6>. Other levels of data are available within the GMOS central database upon request at http://sdi.iaa.cnr.it/geoint/publicpage/GMOS/gmos_historical.zul (GMOS Database, 2014).

Author contribution

K. A. Read, L.J. Carpenter, A. C. Lewis, J. Kentisbeer contributed to the preparation of the manuscript. K. A. Read and L.M. Neves made the measurements. Z. Fleming ran the NAME trajectories and assigned the air mass classifications.

Acknowledgements

The authors acknowledge the Natural Environmental Research Council (NERC) and the Atmospheric Measurement Facility (AMF), National Centre for Atmospheric Science (NCAS) for their continued funding of the Cape Verde Observatory. The measurements of TGM were initiated due to financial support from the EU FP7-ENV-2010 project “Global Mercury observation System” (GMOS, Grant Agreement no 265113).

References

- Ariya, P. A., Sun, J., Eltouny, N. A., Hudson, E. D., Hayes, C. T., and Kos, G.: Physical and chemical characterization of bioaerosols - Implications for nucleation processes, *International Reviews in Physical Chemistry*, 28, 1-32, 10.1080/01442350802597438, 2009.
- Bergan, T., and Rodhe, H.: Oxidation of elemental mercury in the atmosphere; Constraints imposed by global scale modelling, *Journal of Atmospheric Chemistry*, 40, 191-212, 10.1023/a:1011929927896, 2001.
- Bloom, N., and Fitzgerald, W. F.: Determination of Volatile Mercury species at the Picogram level by Low-Temperature Gas Chromatography with Cold-vapour Atomic Fluorescence Detection, *Analytica Chimica Acta*, 208, 151-161, 10.1016/s0003-2670(00)80743-6, 1988.
- Brown, R. J. C., Pirrone, N., van Hoek, C., Horvat, M., Kotnik, J., Wangberg, I., Corns, W. T., Bieber, E., and Sprovieri, F.: Standardisation of a European measurement method for the determination of mercury in deposition: results of the field trial campaign and determination of a measurement uncertainty and working range, *Accreditation and Quality Assurance*, 15, 359-366, 10.1007/s00769-010-0636-2, 2010.
- Calvert, J. G., and Lindberg, S. E.: Mechanisms of mercury removal by O₃ and OH in the atmosphere, *Atmospheric Environment*, 39, 3355-3367, 10.1016/j.atmosenv.2005.01.055, 2005.
- Carpenter, L. J., Fleming, Z. L., Read, K. A., Lee, J. D., Moller, S. J., Hopkins, J. R., Purvis, R. M., Lewis, A. C., Muller, K., Heinold, B., Herrmann, H., Fomba, K. W., van Pinxteren, D., Muller, C., Tegen, I., Wiedensohler, A., Muller, T., Niedermeier, N., Achterberg, E. P., Patey, M. D., Kozlova, E. A., Heimann, M., Heard, D. E., Plane, J. M. C., Mahajan, A., Oetjen, H., Ingham, T., Stone, D., Whalley, L. K., Evans, M. J., Pilling, M. J., Leigh, R. J., Monks, P. S., Karunaharan, A., Vaughan, S., Arnold, S. R., Tschritter, J., Pöhler, D., Friess, U., Holla, R., Mendes, L. M., Lopez, H., Faria, B., Manning, A. J., and Wallace, D. W. R.: Seasonal characteristics of tropical marine boundary layer air measured at the Cape Verde Atmospheric Observatory, *Journal of Atmospheric Chemistry*, 67, 87-140, 10.1007/s10874-011-9206-1, 2010.
- Cinnirella, S., D'Amore, F., Bencardino, M., Sprovieri, F., and Pirrone, N.: The GMOS cyber(e)-infrastructure: advanced services for supporting science and policy, *Environmental Science and Pollution Research*, 21, 4193-4208, 10.1007/s11356-013-2308-3, 2014.



- 1 Cole, A. S., Steffen, A., Eckley, C. S., Narayan, J., Pilote, M., Tordon, R., Graydon, J. A., St Louis, V.
2 L., Xu, X. H., and Branfireun, B. A.: A Survey of Mercury in Air and Precipitation across Canada:
3 Patterns and Trends, *Atmosphere*, 5, 635-668, 10.3390/atmos5030635, 2014.
- 4
5 D'Amore, F., Bencardino, M., Cinnirella, S., Sprovieri, F., and Pirrone, N.: Data quality through a web-
6 based QA/QC system: implementation for atmospheric mercury data from the global mercury
7 observation system, *Environmental Science-Processes & Impacts*, 17, 1482-1491,
8 10.1039/c5em00205b, 2015.
- 9
10 Dastoor, A. P., and Larocque, Y.: Global circulation of atmospheric mercury: a modelling study,
11 *Atmospheric Environment*, 38, 147-161, 10.1016/j.atmosenv.2003.08.037, 2004.
- 12
13 Duncan, B. N., Logan, J. A., Bey, I., Megretskaia, I. A., Yantosca, R. M., Novelli, P. C., Jones, N. B.,
14 and Rinsland, C. P.: Global budget of CO, 1988-1997: Source estimates and validation with a global
15 model, *Journal of Geophysical Research-Atmospheres*, 112, 10.1029/2007jd008459, 2007.
- 16
17 Gay, D. A., Schmeltz, D., Prestbo, E., Olson, M., Sharac, T., and Tordon, R.: The Atmospheric
18 Mercury Network: measurement and initial examination of an ongoing atmospheric mercury record
19 across North America, *Atmospheric Chemistry and Physics*, 13, 11339-11349, 10.5194/acp-13-11339-
20 2013, 2013.
- 21
22 Goodsite, M. E., Plane, J. M. C., and Skov, H.: A theoretical study of the oxidation of Hg-0 to HgBr₂
23 in the troposphere, *Environmental Science & Technology*, 38, 1772-1776, 10.1021/es034680s, 2004.
- 24
25 Gustin, M. S., Weiss-Penzias, P. S., and Peterson, C.: Investigating sources of gaseous oxidized
26 mercury in dry deposition at three sites across Florida, USA, *Atmospheric Chemistry and Physics*, 12,
27 9201-9219, 10.5194/acp-12-9201-2012, 2012.
- 28
29 Holmes, C. D., Jacob, D. J., Corbitt, E. S., Mao, J., Yang, X., Talbot, R., and Slemr, F.: Global
30 atmospheric model for mercury including oxidation by bromine atoms, *Atmospheric Chemistry and
31 Physics*, 10, 12037-12057, 10.5194/acp-10-12037-2010, 2010.
- 32
33 Lan, X., Talbot, R., Castro, M., Perry, K., and Luke, W.: Seasonal and diurnal variations of
34 atmospheric mercury across the US determined from AMNet monitoring data, *Atmospheric Chemistry
35 and Physics*, 12, 10569-10582, 10.5194/acp-12-10569-2012, 2012.
- 36
37 Lin, C. J., Pongprueksa, P., Lindberg, S. E., Pehkonen, S. O., Byun, D., and Jang, C.: Scientific
38 uncertainties in atmospheric mercury models I: Model science evaluation, *Atmospheric Environment*,
39 40, 2911-2928, 10.1016/j.atmosenv.2006.01.009, 2006.
- 40
41 Mason, R. P., Choi, A. L., Fitzgerald, W. F., Hammerschmidt, C. R., Lamborg, C. H., Soerensen, A.
42 L., and Sunderland, E. M.: Mercury biogeochemical cycling in the ocean and policy implications,
43 *Environmental Research*, 119, 101-117, 10.1016/j.envres.2012.03.013, 2012.
- 44
45 Muller, D., Wip, D., Warneke, T., Holmes, C. D., Dastoor, A., and Notholt, J.: Sources of atmospheric
46 mercury in the tropics: continuous observations at a coastal site in Suriname, *Atmospheric Chemistry
47 and Physics*, 12, 7391-7397, 10.5194/acp-12-7391-2012, 2012.
- 48
49 Muntean, M., Janssens-Maenhout, G., Song, S. J., Selin, N. E., Olivier, J. G. J., Guizzardi, D., Maas,
50 R., and Dentener, F.: Trend analysis from 1970 to 2008 and model evaluation of EDGARv4 global
51 gridded anthropogenic mercury emissions, *Science of the Total Environment*, 494, 337-350,
52 10.1016/j.scitotenv.2014.06.014, 2014.
- 53
54 Nair, U. S., Wu, Y. L., Walters, J., Jansen, J., and Edgerton, E. S.: Diurnal and seasonal variation of
55 mercury species at coastal-suburban, urban, and rural sites in the southeastern United States,
56 *Atmospheric Environment*, 47, 499-508, 10.1016/j.atmosenv.2011.09.056, 2012.
- 57
58 Pacyna, E. G., Pacyna, J. M., Sundseth, K., Munthe, J., Kindbom, K., Wilson, S., Steenhuisen, F., and
59 Maxson, P.: Global emission of mercury to the atmosphere from anthropogenic sources in 2005 and



- 1 projections to 2020, *Atmospheric Environment*, 44, 2487-2499, 10.1016/j.atmosenv.2009.06.009,
2 2010.
- 3
- 4 Pirrone, N., Aas, W., Cinnirella, S., Ebinghaus, R., Hedgecock, I. M., Pacyna, J., Sprovieri, F., and
5 Sunderland, E. M.: Toward the next generation of air quality monitoring: Mercury, *Atmospheric*
6 *Environment*, 80, 599-611, 10.1016/j.atmosenv.2013.06.053, 2013.
- 7
- 8 Pongprueksa, P., Lin, C. J., Lindberg, S. E., Jang, C., Braverman, T., Bullock, O. R., Ho, T. C., and
9 Chu, H. W.: Scientific uncertainties in atmospheric mercury models III: Boundary and initial
10 conditions, model grid resolution, and Hg(II) reduction mechanism, *Atmospheric Environment*, 42,
11 1828-1845, 10.1016/j.atmosenv.2007.11.020, 2008.
- 12
- 13 Qureshi, A., MacLeod, M., Sunderland, E. and Hungerbühler, K. (2011) Exchange of Elemental
14 Mercury between the Oceans and the Atmosphere, in *Environmental Chemistry and Toxicology of*
15 *Mercury* (eds G. Liu, Y. Cai and N. O'Driscoll), John Wiley & Sons, Inc., Hoboken, NJ, USA.
16 doi: 10.1002/9781118146644.ch12
- 17
- 18 Read, K. A., Mahajan, A. S., Carpenter, L. J., Evans, M. J., Faria, B. V. E., Heard, D. E., Hopkins, J.
19 R., Lee, J. D., Moller, S. J., Lewis, A. C., Mendes, L., McQuaid, J. B., Oetjen, H., Saiz-Lopez, A.,
20 Pilling, M. J., and Plane, J. M. C.: Extensive halogen-mediated ozone destruction over the tropical
21 Atlantic Ocean, *Nature*, 453, 1232-1235, 10.1038/nature07035, 2008.
- 22
- 23 Read, K. A., Lee, J. D., Lewis, A. C., Moller, S. J., Mendes, L., and Carpenter, L. J.: Intra-annual
24 cycles of NMVOC in the tropical marine boundary layer and their use for interpreting seasonal
25 variability in CO, *Journal of Geophysical Research-Atmospheres*, 114, 10.1029/2009jd011879, 2009.
- 26
- 27 Ryall, D. B., Derwent, R. G., Manning, A. J., Simmonds, P. G., and O'Doherty, S.: Estimating source
28 regions of European emissions of trace gases from observations at Mace Head, *Atmospheric*
29 *Environment*, 35, 2507-2523, 10.1016/s1352-2310(00)00433-7, 2001.
- 30
- 31 Sather, M. E., Mukerjee, S., Smith, L., Mathew, J., Jackson, C., Callison, R., Scrapper, L., Hathcoat,
32 A., Adam, J., Keese, D., Ketcher, P., Brunette, R., Karlstrom, J., and Van der Jagt, G.: Gaseous
33 oxidized mercury dry deposition measurements in the Four Corners area and Eastern Oklahoma,
34 U.S.A, *Atmospheric Pollution Research*, 4, 168-180, 10.5094/apr.2013.017, 2013.
- 35 Schroeder, W. H., and Munthe, J.: Atmospheric mercury - An overview, *Atmospheric Environment*,
36 32, 809-822, 10.1016/s1352-2310(97)00293-8, 1998.
- 37
- 38 Seigneur, C., Vijayaraghavan, K., and Lohman, K.: Atmospheric mercury chemistry: Sensitivity of
39 global model simulations to chemical reactions, *Journal of Geophysical Research-Atmospheres*, 111,
40 10.1029/2005jd006780, 2006.
- 41
- 42 Selin, N. E., Jacob, D. J., Park, R. J., Yantosca, R. M., Strode, S., Jaegle, L., and Jaffe, D.: Chemical
43 cycling and deposition of atmospheric mercury: Global constraints from observations, *Journal of*
44 *Geophysical Research-Atmospheres*, 112, 10.1029/2006jd007450, 2007.
- 45
- 46 Sen, Pranab Kumar: Estimates of the regression coefficient based on Kendall's tau, *Journal of the*
47 *American Statistical Association* 63: 1379-1389, doi:10.2307/2285891, JSTOR 2285891, MR 0258201,
48 1968.
- 49
- 50 Slemr, F., Brunke, E. G., Whittlestone, S., Zahorowski, W., Ebinghaus, R., Kock, H. H., and
51 Labuschagne, C.: Rn-222-calibrated mercury fluxes from terrestrial surface of southern Africa,
52 *Atmospheric Chemistry and Physics*, 13, 6421-6428, 10.5194/acp-13-6421-2013, 2013.
- 53
- 54 Soerensen, A. L., Jacob, D. J., Streets, D. G., Witt, M. L. I., Ebinghaus, R., Mason, R. P., Andersson,
55 M., and Sunderland, E. M.: Multi-decadal decline of mercury in the North Atlantic atmosphere
56 explained by changing subsurface seawater concentrations, *Geophysical Research Letters*, 39,
57 10.1029/2012gl053736, 2012.
- 58



- 1 Sprovieri, F., Pirrone, N., Ebinghaus, R., Kock, H., and Dommergue, A.: A review of worldwide
2 atmospheric mercury measurements, *Atmospheric Chemistry and Physics*, 10, 8245-8265,
3 10.5194/acp-10-8245-2010, 2010.
- 4
- 5 Sprovieri, F., Pirrone, N., Bencardino, M., D'Amore, F., Carbone, F., Cinnirella, S., Mannarino, V.,
6 Landis, M., Ebinghaus, R., Weigelt, A., Brunke, E. G., Labuschagne, C., Martin, L., Munthe, J.,
7 Wangberg, I., Artaxo, P., Morais, F., Barbosa, H. D. J., Brito, J., Cairns, W., Barbante, C., Dieguez, M.
8 D., Garcia, P. E., Dommergue, A., Angot, H., Magand, O., Skov, H., Horvat, M., Kotnik, J., Read, K.
9 A., Neves, L. M., Gawlik, B. M., Sena, F., Mashyanov, N., Obolkin, V., Wip, D., Bin Feng, X., Zhang,
10 H., Fu, X. W., Ramachandran, R., Cossa, D., Knoery, J., Maruszczak, N., Nerentorp, M., and Norstrom,
11 C.: Atmospheric mercury concentrations observed at ground-based monitoring sites globally
12 distributed in the framework of the GMOS network, *Atmospheric Chemistry and Physics*, 16, 11915-
13 11935, 10.5194/acp-16-11915-2016, 2016.
- 14
- 15 Steffen, A., Scherz, T., Olson, M., Gay, D., and Blanchard, P.: A comparison of data quality control
16 protocols for atmospheric mercury speciation measurements, *Journal of Environmental Monitoring*, 14,
17 752-765, 10.1039/c2em10735j, 2012.
- 18
- 19 Steffen, A., Bottenheim, J., Cole, A., Ebinghaus, R., Lawson, G., and Leaitch, W. R.: Atmospheric
20 mercury speciation and mercury in snow over time at Alert, Canada, *Atmospheric Chemistry and*
21 *Physics*, 14, 2219-2231, 10.5194/acp-14-2219-2014, 2014.
- 22
- 23 Streets, D. G., Devane, M. K., Lu, Z. F., Bond, T. C., Sunderland, E. M., and Jacob, D. J.: All-Time
24 Releases of Mercury to the Atmosphere from Human Activities, *Environmental Science &*
25 *Technology*, 45, 10485-10491, 10.1021/es202765m, 2011.
- 26
- 27 Strode, S. A., Jaegle, L., Selin, N. E., Jacob, D. J., Park, R. J., Yantosca, R. M., Mason, R. P., and
28 Slemr, F.: Air-sea exchange in the global mercury cycle, *Global Biogeochemical Cycles*, 21,
29 10.1029/2006gb002766, 2007.
- 30
- 31 Temme, C., Blanchard, P., Steffen, A., Banic, C., Beauchamp, S., Poissant, L., Tordon, R., and Wiens,
32 B.: Trend, seasonal and multivariate analysis study of total gaseous mercury data from the Canadian
33 atmospheric mercury measurement network (CAMNet), *Atmospheric Environment*, 41, 5423-5441,
34 10.1016/j.atmosenv.2007.02.021, 2007.
- 35
- 36 Theil, H.: A rank-invariant method of linear and polynomial regression analysis. I, II, III, *Nederl.*
37 *Akad. Wetensch., Proc.* **53**: 386–392, 521–525, 1397–1412, MR 0036489, 1950.
- 38
- 39 UNEP: UNEP: Technical background report for the Global Mercury Assessment 2013. Arctic
40 Monitoring and Assessment programme, Oslo, Norway/UNEP Chemicals Branch, Geneva,
41 Switzerland, 2013.
- 42
- 43 US EPA: Mercury Study Report to Congress, Fate and transport of mercury in the Environment, vol
44 111, EPA-452/R-97-005, US environmental Protection Agency, US Government Printing Office,
45 Washington, DC, 1997
- 46
- 47 Wang, X., Lin, C. J., and Feng, X.: Sensitivity analysis of an updated bidirectional air-surface
48 exchange model for elemental mercury vapor, *Atmospheric Chemistry and Physics*, 14, 6273-6287,
49 10.5194/acp-14-6273-2014, 2014.
- 50
- 51 Wang, X., Lin, C. J., Lu, Z. Y., Zhang, H., Zhang, Y. P., and Feng, X. B.: Enhanced accumulation and
52 storage of mercury on subtropical evergreen forest floor: Implications on mercury budget in global
53 forest ecosystems, *Journal of Geophysical Research-Biogeosciences*, 121, 2096-2109,
54 10.1002/2016jg003446, 2016.
- 55
- 56 Weigelt, A., Ebinghaus, R., Manning, A. J., Derwent, R. G., Simmonds, P. G., Spain, T. G., Jennings,
57 S. G., and Slemr, F.: Analysis and interpretation of 18 years of mercury observations since 1996 at
58 Mace Head, Ireland, *Atmospheric Environment*, 100, 85-93, 10.1016/j.atmosenv.2014.10.050, 2015.
- 59



- 1 Whalley, L. K., Furneaux, K. L., Goddard, A., Lee, J. D., Mahajan, A., Oetjen, H., Read, K. A.,
2 Kaaden, N., Carpenter, L. J., Lewis, A. C., Plane, J. M. C., Saltzman, E. S., Wiedensohler, A., and
3 Heard, D. E.: The chemistry of OH and HO₂ radicals in the boundary layer over the tropical Atlantic
4 Ocean, *Atmospheric Chemistry and Physics*, 10, 1555-1576, 10.5194/acp-10-1555-2010, 2010.
5
6 Wright, G., Gustin, M. S., Weiss-Penzias, P., and Miller, M. B.: Investigation of mercury deposition
7 and potential sources at six sites from the Pacific Coast to the Great Basin, USA, *Science of the Total*
8 *Environment*, 470, 1099-1113, 10.1016/j.scitotenv.2013.10.071, 2014.
9
10 Zhang, L. M., Wright, L. P., and Blanchard, P.: A review of current knowledge concerning dry
11 deposition of atmospheric mercury, *Atmospheric Environment*, 43, 5853-5864,
12 10.1016/j.atmosenv.2009.08.019, 2009.
13
14 Zhang, Y., Jaegle, L., van Donkelaar, A., Martin, R. V., Holmes, C. D., Amos, H. M., Wang, Q.,
15 Talbot, R., Artz, R., Brooks, S., Luke, W., Holsen, T. M., Felton, D., Miller, E. K., Perry, K. D.,
16 Schmeltz, D., Steffen, A., Tordon, R., Weiss-Penzias, P., and Zsolway, R.: Nested-grid simulation of
17 mercury over North America, *Atmospheric Chemistry and Physics*, 12, 6095-6111, 10.5194/acp-12-
18 6095-2012, 2012.
19
20 Zhang, Y. X., Jacob, D. J., Horowitz, H. M., Chen, L., Amos, H. M., Krabbenhoft, D. P., Slemr, F., St
21 Louis, V. L., and Sunderland, E. M.: Observed decrease in atmospheric mercury explained by global
22 decline in anthropogenic emissions, *Proceedings of the National Academy of Sciences of the United*
23 *States of America*, 113, 526-531, 10.1073/pnas.1516312113, 2016.
24
25
26
27
28
29
30
31
32
33
34
35
36
37
38
39
40
41
42
43
44
45
46
47
48
49
50
51
52
53
54
55
56
57
58
59
60